



THE UNIVERSITY *of* EDINBURGH

Edinburgh Research Explorer

OPEN  ACCESS

Observation of a Narrow Pentaquark State, $P_c(4312)^+$, and of the Two-Peak Structure of the $P_c(4450)^+$

Observation of a Narrow Pentaquark State, $P_c(4312)^+$, and of the Two-Peak Structure of the $P_c(4450)^+$

R. Aaij *et al.**
(LHCb Collaboration)

 (Received 6 April 2019; published 5 June 2019)

A narrow pentaquark state, $P_c(4312)^+$, decaying to $J/\psi p$, is discovered with a statistical significance of 7.3σ in a data sample of $\Lambda_b^0 \rightarrow J/\psi p K^-$ decays, which is an order of magnitude larger than that previously analyzed by the LHCb Collaboration. The $P_c(4450)^+$ pentaquark structure formerly reported by LHCb is confirmed and observed to consist of two narrow overlapping peaks, $P_c(4440)^+$ and $P_c(4457)^+$, where the statistical significance of this two-peak interpretation is 5.4σ . The proximity of the $\Sigma_c^+ \bar{D}^0$ and $\Sigma_c^+ \bar{D}^{*0}$ thresholds to the observed narrow peaks suggests that they play an important role in the dynamics of these states.

DOI: 10.1103/PhysRevLett.122.222001

A major turning point in exotic baryon spectroscopy was achieved at the Large Hadron Collider when, from an analysis of Run 1 data, the LHCb Collaboration reported the observation of significant $J/\psi p$ pentaquark structures in $\Lambda_b^0 \rightarrow J/\psi p K^-$ decays (inclusion of charge-conjugate processes is implied throughout). A model-dependent six-dimensional amplitude analysis of invariant masses and decay angles describing the Λ_b^0 decay revealed a $P_c(4450)^+$ structure peaking at $4449.8 \pm 1.7 \pm 2.5$ MeV with a width of $39 \pm 5 \pm 19$ MeV and a fit fraction of $(4.1 \pm 0.5 \pm 1.1)\%$ [1]. Even though not apparent from the $m_{J/\psi p}$ distribution alone, the amplitude analysis also required a second broad $J/\psi p$ state to obtain a good description of the data, which peaks at $4380 \pm 8 \pm 29$ MeV with a width of $205 \pm 18 \pm 86$ MeV and a fit fraction of $(8.4 \pm 0.7 \pm 4.2)\%$. Furthermore, the exotic hadron character of the $J/\psi p$ structure near 4450 MeV was demonstrated in a model-independent way in Ref. [2], where it was shown to be too narrow to be accounted for by $\Lambda^* \rightarrow p K^-$ reflections (Λ^* denotes Λ excitations). Various interpretations of these structures have been proposed, including tightly bound $duuc\bar{c}$ pentaquark states [3–9], loosely bound molecular baryon-meson pentaquark states [10–15], or peaks due to triangle-diagram processes [16–19].

In this Letter, an analysis is presented of $\Lambda_b^0 \rightarrow J/\psi p K^-$ decays based on the combined dataset collected by the LHCb Collaboration in Run 1, with pp collision energies of 7 and 8 TeV corresponding to a total integrated

luminosity of 3 fb^{-1} , and in Run 2 at 13 TeV corresponding to 6 fb^{-1} . The LHCb detector is a single-arm forward spectrometer covering the pseudorapidity range $2 < \eta < 5$, described in detail in Refs. [20,21]. The data selection is similar to that used in Ref. [1]. However, in this updated analysis, the hadron identification information is included in the boosted decision tree (BDT) discriminant, which increases the Λ_b^0 signal efficiency by almost a factor of 2 while leaving the background level almost unchanged. The resulting sample contains 246000 $\Lambda_b^0 \rightarrow J/\psi p K^-$ decays (see the Supplemental Material to this Letter [22]), which is nine times more than was used in the Run 1 analyses [1,2].

When this combined dataset is fit with the same amplitude model used in Ref. [1], the $P_c(4450)^+$ and $P_c(4380)^+$ parameters are found to be consistent with the previous results. However, this should be considered only as a cross check, since analysis of this much larger data sample reveals additional peaking structures in the $J/\psi p$ mass spectrum, which are too small to have been significant before (see left plot of Fig. 1). A narrow peak is observed near 4312 MeV with a width comparable to the mass resolution. The structure at 4450 MeV is now resolved into

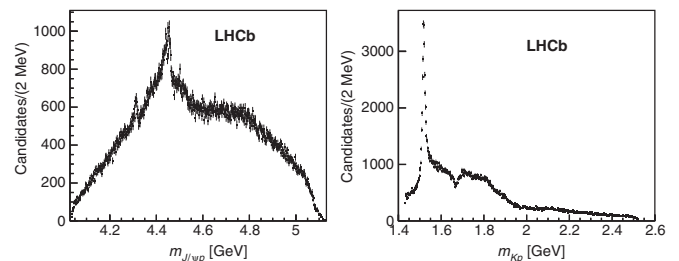


FIG. 1. Distribution of (left) $m_{J/\psi p}$ and (right) m_{Kp} for $\Lambda_b^0 \rightarrow J/\psi p K^-$ candidates. The prominent peak in m_{Kp} is due to the $\Lambda(1520)$ resonance.

*Full author list given at the end of the Letter.

Published by the American Physical Society under the terms of the Creative Commons Attribution 4.0 International license. Further distribution of this work must maintain attribution to the author(s) and the published article's title, journal citation, and DOI. Funded by SCOAP³.

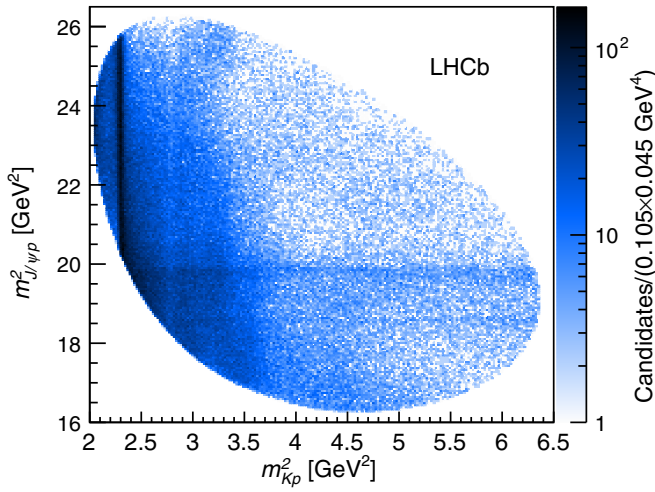


FIG. 2. Dalitz plot of $\Lambda_b^0 \rightarrow J/\psi p K^-$ candidates. The data contain 6.4% of non- Λ_b^0 backgrounds, which are distributed smoothly over the phase space. The vertical bands correspond to the Λ^* resonances. The horizontal bands correspond to the $P_c(4312)^+$, $P_c(4440)^+$, and $P_c(4457)^+$ structures at $m_{J/\psi p}^2 = 18.6, 19.7, \text{ and } 19.9 \text{ GeV}^2$, respectively.

two narrow peaks at 4440 and 4457 MeV, which are more visible when the dominant $\Lambda^* \rightarrow p K^-$ contributions, which peak at low $p K^-$ masses (m_{Kp}), as shown in the right plot of Fig. 1 and in Fig. 2, are suppressed by requiring $m_{Kp} > 1.9 \text{ GeV}$ (see Fig. 3). This m_{Kp} requirement maximizes the expected signal significance for P_c^+ states that decay isotropically.

Performing a rigorous amplitude analysis of this new data sample is computationally challenging. The $m_{J/\psi p}$ mass resolution must be taken into account, and the size of the data sample to fit has greatly increased. Formulating an amplitude model whose systematic uncertainties are comparable to the statistical precision provided by this larger data sample is difficult given the large number of Λ^* excitations [26,27] and coupled-channel effects [28], and the possible presence of one or more wide P_c^+ contributions, like the previously reported $P_c(4380)^+$ state. Fortunately, the newly observed peaks are so narrow that it is not necessary to construct an amplitude model to prove that these states are not artifacts of interfering Λ^* resonances [2].

Binned χ^2 fits are performed to the one-dimensional $m_{J/\psi p}$ distribution in the range $4.22 < m_{J/\psi p} < 4.57 \text{ GeV}$ to determine the masses (M), widths (Γ), and relative production rates (\mathcal{R}) of the narrow P_c^+ states under the assumption that they can be described by relativistic Breit-Wigner (BW) amplitudes. These $m_{J/\psi p}$ fits alone cannot distinguish broad P_c^+ states from other contributions that vary slowly with $m_{J/\psi p}$. Therefore, a verification of the $P_c(4380)^+$ state observed in Ref. [1] awaits completion of an amplitude analysis of this new larger dataset.

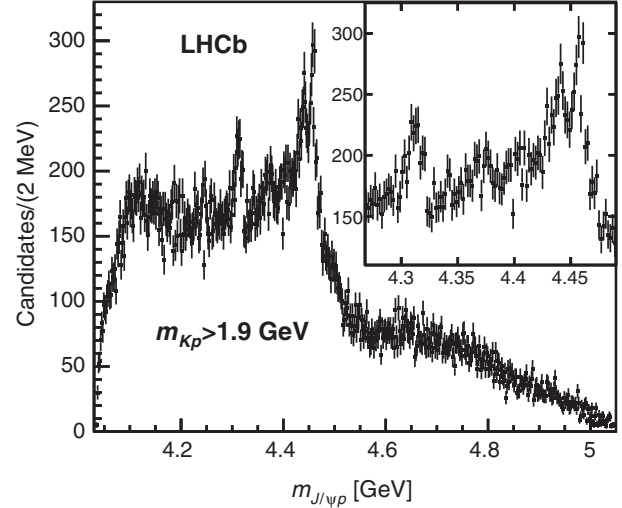


FIG. 3. Distribution of $m_{J/\psi p}$ from $\Lambda_b^0 \rightarrow J/\psi p K^-$ candidates after suppression of the dominant $\Lambda^* \rightarrow p K^-$ contributions with the $m_{Kp} > 1.9 \text{ GeV}$ requirement. The inset shows a zoom into the region of the narrow P_c^+ peaks.

Many variations of the $m_{J/\psi p}$ fits are performed to study the robustness of the measured P_c^+ properties. The $m_{J/\psi p}$ distribution is fit both with and without requiring $m_{Kp} > 1.9 \text{ GeV}$, which removes over 80% of the Λ^* contributions. In addition, fits are performed on the $m_{J/\psi p}$ distribution obtained by applying $\cos \theta_{P_c}$ -dependent weights to each candidate to enhance the P_c^+ signal, where θ_{P_c} is the angle between the K^- and J/ψ in the P_c^+ rest frame (the P_c^+ helicity angle [1]). The Λ^* contributions mostly populate the $\cos \theta_{P_c} > 0$ region. The weights are taken to be the inverse of the expected background at each $\cos \theta_{P_c}$, which is approximately given by the density of candidates observed in data since the signal contributions are small. The weight function is shown in Fig. 4. The best sensitivity to P_c^+ contributions is obtained from the $\cos \theta_{P_c}$ -weighted $m_{J/\psi p}$ distribution, followed by the sample with the $m_{Kp} > 1.9 \text{ GeV}$ requirement. However, since the background composition and shape are different in the three

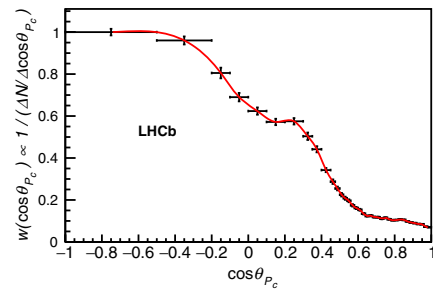


FIG. 4. Weight function $w(\cos \theta_{P_c})$ applied to candidates, determined as the inverse of the density of Λ_b^0 candidates in the narrow P_c^+ peak region. The red line is a spline function used to interpolate between bin centers.

samples, the results from all three fits are used when assessing the systematic uncertainties.

The one-dimensional fit strategy is validated on ensembles of large simulated datasets sampled from several six-dimensional amplitude models, similar to those of Ref. [1], with or without a broad P_c^+ state and considering various P_c^+ quantum number assignments. The main conclusion from these studies is that the dominant systematic uncertainty is due to possible interference between various P_c^+ states. Such interference effects cannot be unambiguously disentangled using the $m_{J/\psi p}$ distribution alone. Therefore, fits are performed considering many possible interference configurations, with the observed variations in the P_c^+ properties assigned as systematic uncertainties.

In all fits, the $m_{J/\psi p}$ distribution is modeled by three narrow BW P_c^+ terms and a smooth parametrization of the background. Here, background refers to Λ^* reflections, small non- Λ_b^0 contributions (which comprise 6.4% of the sample), and possibly additional broad P_c^+ structures. Many different background parametrizations are considered (discussed below), each of which is found to produce negligible bias in the P_c^+ parameters in the validation fits. Each fit component is multiplied by a phase-space factor, $p \cdot q$, where p (q) is the breakup momentum in the $\Lambda_b^0 \rightarrow P_c^+ K^-$ ($P_c^+ \rightarrow J/\psi p$) decay. Since the signal peaks are narrow, all fit components are convolved with the detector resolution, which is 2–3 MeV in the fit region (see the Supplemental Material [22]). Finally, the detection efficiency has negligible impact on the signal $m_{J/\psi p}$ distributions, and therefore is not considered in these fits.

In the nominal fits, the BW contributions are added incoherently. The results of these fits are displayed in Fig. 5 for two parametrizations of the background: one using a high-order polynomial; and another using a low-order polynomial, along with an additional wide P_c^+ BW term whose mass and width are free to vary in the fits. For both background parametrizations, a range of polynomial orders is considered. The lowest order used for each case is the smallest that adequately describes the data, which is found to correspond to the minimum order required to obtain unbiased P_c^+ estimators in the fit-validation studies in the absence of interference. The highest orders are chosen such that the background model is capable of describing any structures that could be produced by either non- P_c^+ or broad- P_c^+ contributions. Figure 6 shows the fit from which the central values of the P_c^+ properties are obtained, while the background-model-dependent variations observed in these properties are included in the systematic uncertainties. The fits with and without the broad P_c^+ state both describe the data well. Therefore, these fits can neither confirm nor contradict the existence of the $P_c(4380)^+$ state.

To determine the significance of the $P_c(4312)^+$ state, the change of the fit χ^2 when adding this component is used as the test statistic, where the distribution under the null

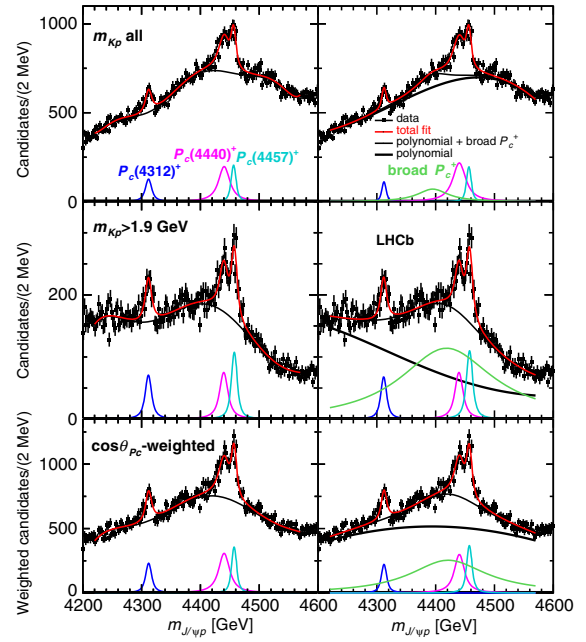


FIG. 5. Fits to the $m_{J/\psi p}$ distributions of the (top row) inclusive, (middle row) $m_{Kp} > 1.9$ GeV, and (bottom row) $\cos \theta_{pc}$ -weighted samples with three incoherently summed BW amplitudes representing the narrow P_c^+ signals on top of a (left column) high-order polynomial function or (right column) lower-order polynomial plus a broad P_c^+ state represented by a fourth BW amplitude.

hypothesis is obtained from a large ensemble of pseudoexperiments. The p value, expressed in Gaussian standard deviations, corresponds to 7.6σ (8.5σ) for the fits to the $m_{Kp} > 1.9$ GeV ($\cos \theta_{pc}$ -weighted) distribution, ignoring the look-elsewhere effect. To account for this effect, the $m_{J/\psi p}$ distribution in each pseudoexperiment is scanned to find the most significant narrow and isolated peak (excluding the 4450 MeV peak region). This method lowers the $P_c(4312)^+$ significance to 7.3σ (8.2σ).

To evaluate the significance of the two-peak structure versus the one-peak interpretation of the 4450 MeV region, the null hypothesis uses just one BW to encompass both the $P_c(4440)^+$ and $P_c(4457)^+$ peaks [the fit also includes the $P_c(4312)^+$ BW], which gives $P_c(4450)^+$ mass and width values that are consistent with those obtained from the amplitude analysis of Ref. [1]. Pseudoexperiments are again used to determine the $\Delta\chi^2$ distribution under the null hypothesis. The significance of the two-peak structure is 5.4σ (6.2σ) for the $m_{Kp} > 1.9$ GeV ($\cos \theta_{pc}$ -weighted) samples. This significance is large enough to render the single-peak interpretation of the 4450 MeV region obsolete. Therefore, the results presented here for this structure supersede those previously presented in Ref. [1] (see the Supplemental Material for more detailed discussion [22]). To investigate the systematic uncertainties on P_c^+ properties due to interference, which can only be important for P_c^+

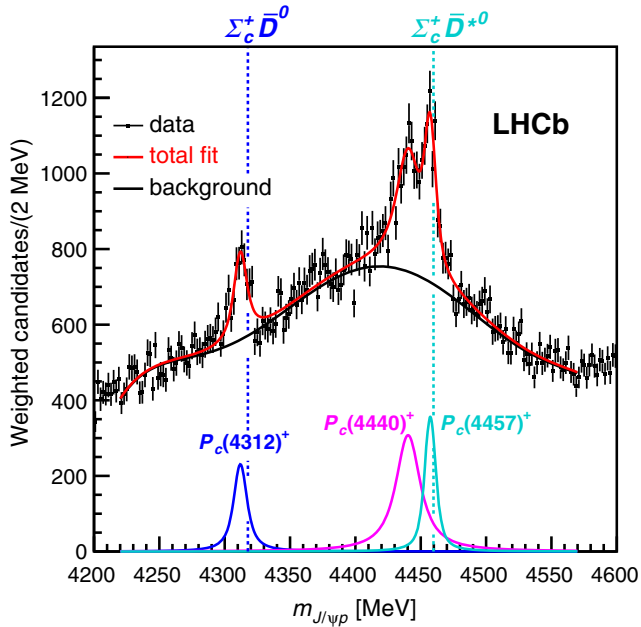


FIG. 6. Fit to the $\cos\theta_{P_c}$ -weighted $m_{J/\psi p}$ distribution with three BW amplitudes and a sixth-order polynomial background. This fit is used to determine the central values of the masses and widths of the P_c^+ states. The mass thresholds for the $\Sigma_c^+ \bar{D}^0$ and $\Sigma_c^+ \bar{D}^{*0}$ final states are superimposed.

resonances with the same spin and parity, fits to the $\cos\theta_{P_c}$ -weighted distribution are repeated using various coherent sums of two of the BW amplitudes. Each of these fits includes a phase between interfering resonances as an extra free parameter. None of the interference effects studied is found to produce a significant $\Delta\chi^2$ relative to the fits using an incoherent sum of BW amplitudes. However, substantial shifts in the P_c^+ properties are observed, and are included in the systematic uncertainties. For example, in such a fit the $P_c(4312)^+$ mass increases, while its width is rather stable, leading to a large positive systematic uncertainty of 6.8 MeV on its mass.

As in Ref. [1], the Λ_b^0 candidates are kinematically constrained to the known J/ψ and Λ_b^0 masses [29], which substantially improves the $m_{J/\psi p}$ resolution and determines the absolute mass scale with an accuracy of 0.2 MeV. The mass resolution is known with a 10% relative uncertainty. Varying this within its uncertainty changes the widths of the narrow states in the nominal fit by up to 0.5 MeV, 0.2 MeV, and 0.8 MeV for the $P_c(4312)^+$,

$P_c(4440)^+$, and $P_c(4457)^+$ states, respectively. The widths of all three narrow P_c^+ peaks are consistent with the mass resolution within the systematic uncertainties. Therefore, upper limits are placed on their natural widths at the 95% confidence level (C.L.), which account for the uncertainty on the detector resolution and in the fit model.

A number of additional fits are performed when evaluating the systematic uncertainties. The nominal fits assume S -wave (no angular momentum) production and decay. Including P -wave factors in the BW amplitudes has negligible effect on the results. In addition to the nominal fits with three narrow peaks in the $4.22 < m_{J/\psi p} < 4.57$ GeV region, fits including only the $P_c(4312)^+$ are performed in the narrow 4.22–4.44 GeV range. Fits are also performed using a data sample selected with an alternative approach, where no BDT is used, resulting in about twice as much background.

The total systematic uncertainties assigned on the mass and width of each narrow P_c^+ state are taken to be the largest deviations observed among all fits. These include the fits to all three versions of the $m_{J/\psi p}$ distribution, each configuration of the P_c^+ interference, all variations of the background model, and each of the additional fits just described. The masses, widths, and relative contributions (\mathcal{R} values) of the three narrow P_c^+ states, including all systematic uncertainties, are given in Table I.

To obtain estimates of the relative contributions of the P_c^+ states, the Λ_b^0 candidates are weighted by the inverse of the reconstruction efficiency, which is parametrized in all six dimensions of the Λ_b^0 decay phase space [Eq. (68) in the Supplemental Material to Ref. [30]]. The efficiency-weighted $m_{J/\psi p}$ distribution, without the $m_{Kp} > 1.9$ GeV requirement, is fit to determine the P_c^+ contributions, which are then divided by the efficiency-corrected and background-subtracted Λ_b^0 yields. This method makes the results independent of the unknown quantum numbers and helicity structure of the P_c^+ production and decay. Unfortunately, this approach also suffers from large Λ^* backgrounds and from sizable fluctuations in the low-efficiency regions. In these fits, the P_c^+ terms are added incoherently, absorbing any interference effects, which can be large (see, e.g., Fig. S2 in the Supplemental Material [22]), into the BW amplitudes. Therefore, the $\mathcal{R} \equiv \mathcal{B}(\Lambda_b^0 \rightarrow P_c^+ K^-) \mathcal{B}(P_c^+ \rightarrow J/\psi p) / \mathcal{B}(\Lambda_b^0 \rightarrow J/\psi p K^-)$ values reported for each P_c^+ state differ from the fit fractions

TABLE I. Summary of P_c^+ properties. The central values are based on the fit displayed in Fig. 6.

State	M [MeV]	Γ [MeV]	(95% C.L.)	\mathcal{R} [%]
$P_c(4312)^+$	$4311.9 \pm 0.7^{+6.8}_{-0.6}$	$9.8 \pm 2.7^{+3.7}_{-4.5}$	(<27)	$0.30 \pm 0.07^{+0.34}_{-0.09}$
$P_c(4440)^+$	$4440.3 \pm 1.3^{+4.1}_{-4.7}$	$20.6 \pm 4.9^{+8.7}_{-10.1}$	(<49)	$1.11 \pm 0.33^{+0.22}_{-0.10}$
$P_c(4457)^+$	$4457.3 \pm 0.6^{+4.1}_{-1.7}$	$6.4 \pm 2.0^{+5.7}_{-1.9}$	(<20)	$0.53 \pm 0.16^{+0.15}_{-0.13}$

typically reported in amplitude analyses, since \mathcal{R} includes both the BW amplitude squared and all of its interference terms. Similar fit variations are considered here as above; e.g., different background models and selection criteria are all evaluated. The resulting systematic uncertainties on \mathcal{R} are large, as shown in Table I.

The narrow widths of the P_c^+ peaks make a compelling case for the bound-state character of the observed states. However, it has been pointed out by many authors [16–19] that peaking structures in this $J/\psi p$ mass range can also be generated by triangle diagrams. The $P_c(4312)^+$ and $P_c(4440)^+$ peaks are unlikely to arise from triangle diagrams, due to a lack of any appropriate hadron-rescattering thresholds, as discussed in more detail in the Supplemental Material [22]. The $P_c(4457)^+$ peaks at the $\Lambda_c^+(2595)\bar{D}^0$ threshold ($J^P = 1/2^+$ in S -wave) [18], and the $D_{s1}(2860)^-$ meson is a suitable candidate to be exchanged in the corresponding triangle diagram. However, this triangle-diagram term does not describe the data nearly as well as the BW does (see Fig. S5 in the Supplemental Material [22]). This possibility deserves more scrutiny within the amplitude analysis approach.

Narrow P_c^+ states could arise by binding a narrow baryon with a narrow meson, where the separation of c and \bar{c} into distinct confinement volumes provides a natural suppression mechanism for the P_c^+ widths. The only narrow baryon-meson combinations with mass thresholds in the appropriate mass range are $p\chi_{cJ}$, $\Lambda_c^+\bar{D}^{(*)0}$, and $\Sigma_c\bar{D}^{(*)}$ (both $\Sigma_c^+\bar{D}^{(*)0}$ and $\Sigma_c^+\bar{D}^{(*)-}$ are possible; the threshold for the latter is about 5 MeV higher than the former). There is no known S -wave binding mechanism for $p\chi_{cJ}$ combinations [31], and $\Lambda_c^+\bar{D}^{(*)0}$ interactions are expected to be repulsive, leaving only the $\Sigma_c\bar{D}^{(*)}$ pairs expected to form bound states [32–34]. The masses of the $P_c(4312)^+$ and $P_c(4457)^+$ states are approximately 5 MeV and 2 MeV below the $\Sigma_c^+\bar{D}^0$ and $\Sigma_c^+\bar{D}^{*0}$ thresholds, respectively, as illustrated in Fig. 6, making them excellent candidates for bound states of these systems. The $P_c(4440)^+$ could be the second $\Sigma_c\bar{D}^*$ state, with about 20 MeV of binding energy, since two states with $J^P = 1/2^-$ and $3/2^-$ are possible. In fact, several papers on hidden-charm states created dynamically by charmed meson-baryon interactions [35–37] were published well before the first observation of the P_c^+ structures [1], and some of these predictions for $\Sigma_c^+\bar{D}^0$ and $\Sigma_c^+\bar{D}^{*0}$ states [32–34] are consistent with the observed narrow P_c^+ states. Such an interpretation of the $P_c(4312)^+$ state (implies $J^P = 1/2^-$) would point to the importance of ρ -meson exchange, since a pion cannot be exchanged in this system [10].

In summary, the ninefold increase in the number of $\Lambda_b^0 \rightarrow J/\psi p K^-$ decays reconstructed with the LHCb detector sheds more light onto the $J/\psi p$ structures found in this final state. The previously reported $P_c(4450)^+$ peak [1] is confirmed and resolved at 5.4σ significance into two

narrow states: the $P_c(4440)^+$ and $P_c(4457)^+$ exotic baryons. A narrow companion state, $P_c(4312)^+$, is discovered with 7.3σ significance.

The minimal quark content of these states is $duuc\bar{c}$. Since all three states are narrow and below the $\Sigma_c^+\bar{D}^0$ and $\Sigma_c^+\bar{D}^{*0}$ ($[duc][u\bar{c}]$) thresholds within plausible hadron-hadron binding energies, they provide the strongest experimental evidence to date for the existence of bound states of a baryon and a meson. The $\Sigma_c^+\bar{D}^0$ ($\Sigma_c^+\bar{D}^{*0}$) threshold is within the extent of the $P_c(4312)^+$ [$P_c(4457)^+$] peak, and therefore virtual [38] rather than bound states are among the plausible explanations. In simple tightly bound pentaquark models, the proximity of these states to baryon-meson thresholds would be coincidental, and furthermore, it is difficult to accommodate their narrow widths [39]. A potential barrier between diquarks, which could separate the c and \bar{c} quarks, has been proposed to solve similar difficulties for tetraquark candidates [40]. An interplay between tightly bound pentaquarks and the $\Sigma_c\bar{D}$, $\Sigma_c\bar{D}^*$ thresholds may also be responsible for the P_c^+ peaks [41–44]. Therefore, such alternative explanations cannot be ruled out. Proper identification of the internal structure of the observed states will require more experimental and theoretical scrutiny.

We express our gratitude to our colleagues in the CERN accelerator departments for the excellent performance of the LHC. We thank the technical and administrative staff at the LHCb institutes. We acknowledge support from CERN and from the national agencies: CAPES, CNPq, FAPERJ, and FINEP (Brazil); MOST and NSFC (China); CNRS/IN2P3 (France); BMBF, DFG, and MPG (Germany); INFN (Italy); NWO (Netherlands); MNiSW and NCN (Poland); MEN/IFA (Romania); MSHE (Russia); MinECo (Spain); SNSF and SER (Switzerland); NASU (Ukraine); STFC (United Kingdom); NSF (USA). We acknowledge the computing resources that are provided by CERN, IN2P3 (France), KIT and DESY (Germany), INFN (Italy), SURF (Netherlands), PIC (Spain), GridPP (United Kingdom), RRCKI and Yandex LLC (Russia), CSCS (Switzerland), IFIN-HH (Romania), CBPF (Brazil), PL-GRID (Poland) and OSC (USA). We are indebted to the communities behind the multiple open-source software packages on which we depend. Individual groups or members have received support from the AvH Foundation (Germany); EPLANET, Marie Skłodowska-Curie Actions and ERC (European Union); ANR, Labex P2IO and OCEVU, and Région Auvergne-Rhône-Alpes (France); the Key Research Program of Frontier Sciences of CAS, CAS PIFI, and the Thousand Talents Program (China); RFBR, RSF and Yandex LLC (Russia); GVA, XuntaGal and GENCAT (Spain); the Royal Society and the Leverhulme Trust (United Kingdom); the Laboratory Directed Research and Development program of LANL (USA); and CONACYT (Mexico).

- [1] R. Aaij *et al.* (LHCb Collaboration), Observation of $J/\psi p$ Resonances Consistent with Pentaquark States in $\Lambda_b^0 \rightarrow J/\psi p K^-$ Decays, *Phys. Rev. Lett.* **115**, 072001 (2015).
- [2] R. Aaij *et al.* (LHCb Collaboration), Model-Independent Evidence for $J/\psi p$ Contributions to $\Lambda_b^0 \rightarrow J/\psi p K^-$ Decays, *Phys. Rev. Lett.* **117**, 082002 (2016).
- [3] L. Maiani, A. D. Polosa, and V. Riquer, The new pentaquarks in the diquark model, *Phys. Lett. B* **749**, 289 (2015).
- [4] R. F. Lebed, The pentaquark candidates in the dynamical diquark picture, *Phys. Lett. B* **749**, 454 (2015).
- [5] V. V. Anisovich *et al.*, Pentaquarks and resonances in the pJ/ψ spectrum, arXiv:1507.07652.
- [6] G.-N. Li, X.-G. He, and M. He, Some predictions of diquark model for hidden charm pentaquark discovered at the LHCb, *J. High Energy Phys.* **12** (2015) 128.
- [7] R. Ghosh, A. Bhattacharya, and B. Chakrabarti, A study on $P_c^*(4380)$ and $P_c^*(4450)$ in the quasiparticle diquark model, *Phys. Part. Nucl. Lett.* **14**, 550 (2017).
- [8] Z.-G. Wang, Analysis of $P_c(4380)$ and $P_c(4450)$ as pentaquark states in the diquark model with QCD sum rules, *Eur. Phys. J. C* **76**, 70 (2016).
- [9] R. Zhu and C.-F. Qiao, Pentaquark states in a diquark-triquark model, *Phys. Lett. B* **756**, 259 (2016).
- [10] M. Karliner and J. L. Rosner, New Exotic Meson and Baryon Resonances from Doubly-Heavy Hadronic Molecules, *Phys. Rev. Lett.* **115**, 122001 (2015).
- [11] R. Chen, X. Liu, X.-Q. Li, and S.-L. Zhu, Identifying Exotic Hidden-Charm Pentaquarks, *Phys. Rev. Lett.* **115**, 132002 (2015).
- [12] H.-X. Chen, W. Chen, X. Lu, T. G. Steele, and S.-L. Zhu, Towards Exotic Hidden-Charm Pentaquarks in QCD, *Phys. Rev. Lett.* **115**, 172001 (2015).
- [13] L. Roca, J. Nieves, and E. Oset, LHCb pentaquark as a $\bar{D}^* \Sigma_c - \bar{D}^* \Sigma_c^*$ molecular state, *Phys. Rev. D* **92**, 094003 (2015).
- [14] J. He, $\bar{D} \Sigma_c^*$ and $\bar{D}^* \Sigma_c$ interactions and the LHCb hidden-charmed pentaquarks, *Phys. Lett. B* **753**, 547 (2016).
- [15] H. Huang, C. Deng, J. Ping, and F. Wang, Possible pentaquarks with heavy quarks, *Eur. Phys. J. C* **76**, 624 (2016).
- [16] F.-K. Guo, U.-G. Meißner, W. Wang, and Z. Yang, How to reveal the exotic nature of the $P_c(4450)$, *Phys. Rev. D* **92**, 071502(R) (2015).
- [17] U.-G. Meißner and J. A. Oller, Testing the $\chi_{c1} P$ composite nature of the $P_c(4450)$, *Phys. Lett. B* **751**, 59 (2015).
- [18] X.-H. Liu, Q. Wang, and Q. Zhao, Understanding the newly observed heavy pentaquark candidates, *Phys. Lett. B* **757**, 231 (2016).
- [19] M. Mikhasenko, A triangle singularity and the LHCb pentaquarks, arXiv:1507.06552.
- [20] A. A. Alves, Jr. *et al.* (LHCb Collaboration), The LHCb detector at the LHC, *J. Instrum.* **3**, S08005 (2008).
- [21] R. Aaij *et al.* (LHCb Collaboration), LHCb detector performance, *Int. J. Mod. Phys. A* **30**, 1530022 (2015).
- [22] See Supplemental Material at <http://link.aps.org/supplemental/10.1103/PhysRevLett.122.222001> for additional information, illustrations and study of triangle diagrams, which includes Refs. [23–25].
- [23] A. P. Szczepaniak, Dalitz plot distributions in presence of triangle singularities, *Phys. Lett. B* **757**, 61 (2016).
- [24] R. Aaij *et al.* (LHCb Collaboration), Observation of Overlapping Spin-1 and Spin-3 $\bar{D}^0 K^-$ Resonances at Mass 2.86 GeV/ c^2 , *Phys. Rev. Lett.* **113**, 162001 (2014).
- [25] S. Godfrey and K. Moats, Properties of excited charm and charm-strange mesons, *Phys. Rev. D* **93**, 034035 (2016).
- [26] S. Capstick and N. Isgur, Baryons in a relativized quark model with chromodynamics, *Phys. Rev. D* **34**, 2809 (1986).
- [27] U. Loring, B. C. Metsch, and H. R. Petry, The light-baryon spectrum in a relativistic quark model with instanton induced quark forces: The strange baryon spectrum, *Eur. Phys. J. A* **10**, 447 (2001).
- [28] C. Fernandez-Ramirez, I. V. Danilkin, D. M. Manley, V. Mathieu, and A. P. Szczepaniak (Joint Physics Analysis Center), Coupled-channel model for $\bar{K}N$ scattering in the resonant region, *Phys. Rev. D* **93**, 034029 (2016).
- [29] M. Tanabashi *et al.* (Particle Data Group), Review of particle physics, *Phys. Rev. D* **98**, 030001 (2018).
- [30] R. Aaij *et al.* (LHCb Collaboration), Search for Structure in the $B_s^0 \pi^\pm$ Invariant Mass Spectrum, *Phys. Rev. Lett.* **117**, 152003 (2016).
- [31] T. J. Burns, Phenomenology of $P_c(4380)^+$, $P_c(4450)^+$ and related states, *Eur. Phys. J. A* **51**, 152 (2015).
- [32] W. L. Wang, F. Huang, Z. Y. Zhang, and B. S. Zou, $\Sigma_c \bar{D}$ and $\Lambda_c^+ \bar{D}$ states in a chiral quark model, *Phys. Rev. C* **84**, 015203 (2011).
- [33] Z.-C. Yang, Z.-F. Sun, J. He, X. Liu, and S.-L. Zhu, Possible hidden-charm molecular baryons composed of anti-charmed meson and charmed baryon, *Chin. Phys. C* **36**, 6 (2012).
- [34] J.-J. Wu, T.-S. H. Lee, and B. S. Zou, Nucleon resonances with hidden charm in coupled-channel models, *Phys. Rev. C* **85**, 044002 (2012).
- [35] J.-J. Wu, R. Molina, E. Oset, and B. S. Zou, Prediction of Narrow N^* and Λ^* Resonances with Hidden Charm above 4 GeV, *Phys. Rev. Lett.* **105**, 232001 (2010).
- [36] J.-J. Wu, R. Molina, E. Oset, and B. S. Zou, Dynamically generated N^* and Λ^* resonances in the hidden charm sector around 4.3 GeV, *Phys. Rev. C* **84**, 015202 (2011).
- [37] C. W. Xiao, J. Nieves, and E. Oset, Combining heavy quark spin and local hidden gauge symmetries in the dynamical generation of hidden charm baryons, *Phys. Rev. D* **88**, 056012 (2013).
- [38] W. R. Frazer and A. W. Hendry, S -matrix poles close to threshold, *Phys. Rev.* **134**, B1307 (1964).
- [39] E. Hiyama, A. Hosaka, M. Oka, and J.-M. Richard, Quark model estimate of hidden-charm pentaquark resonances, *Phys. Rev. C* **98**, 045208 (2018).
- [40] L. Maiani, A. D. Polosa, and V. Riquer, A theory of X and Z multi-quark resonances, *Phys. Lett. B* **778**, 247 (2018).
- [41] D. V. Bugg, How resonances can synchronise with thresholds, *J. Phys. G* **35**, 075005 (2008).
- [42] F.-K. Guo, C. Hanhart, Q. Wang, and Q. Zhao, Could the near-threshold XYZ states be simply kinematic effects? *Phys. Rev. D* **91**, 051504(R) (2015).

- [43] S. H. Blitz and R. F. Lebed, Tetraquark cusp effects from diquark pair production, *Phys. Rev. D* **91**, 094025 (2015).
- [44] F.-K. Guo, C. Hanhart, Yu. S. Kalashnikova, P. Matuschek, R. V. Mizuk, A. V. Nefediev, Q. Wang, and J.-L. Wymen, Interplay of quark and meson degrees of freedom in near-threshold states: A practical parametrization for line shapes, *Phys. Rev. D* **93**, 074031 (2016).
-
- R. Aaij,²⁸ C. Abellán Beteta,⁴⁶ B. Adeva,⁴³ M. Adinolfi,⁵⁰ C. A. Aidala,⁷⁹ Z. Ajaltouni,⁶ S. Akar,⁶¹ P. Albicocco,¹⁹ J. Albrecht,¹¹ F. Alessio,⁴⁴ M. Alexander,⁵⁵ A. Alfonso Alberro,⁴² G. Alkhazov,⁴¹ P. Alvarez Cartelle,⁵⁷ A. A. Alves Jr.,⁴³ S. Amato,² Y. Amhis,⁸ L. An,¹⁸ L. Anderlini,¹⁸ G. Andreassi,⁴⁵ M. Andreotti,¹⁷ J. E. Andrews,⁶² F. Archilli,¹⁹ P. d'Argent,¹³ J. Arnau Romeu,⁷ A. Artamonov,⁴⁰ M. Artuso,⁶³ K. Arzymatov,³⁷ E. Aslanides,⁷ M. Atzeni,⁴⁶ B. Audurier,²³ S. Bachmann,¹³ J. J. Back,⁵² S. Baker,⁵⁷ V. Balagura,^{8,a} W. Baldini,^{17,44} A. Baranov,³⁷ R. J. Barlow,⁵⁸ S. Barsuk,⁸ W. Barter,⁵⁷ M. Bartolini,²⁰ F. Baryshnikov,⁷⁶ V. Batozskaya,³² B. Batsukh,⁶³ A. Battig,¹¹ V. Battista,⁴⁵ A. Bay,⁴⁵ F. Bedeschi,²⁵ I. Bediaga,¹ A. Beiter,⁶³ L. J. Bel,²⁸ V. Belavin,³⁷ S. Belin,²³ N. Belyi,⁶⁶ V. Bellee,⁴⁵ N. Belloli,^{21,b} K. Belous,⁴⁰ I. Belyaev,³⁴ E. Ben-Haim,⁹ G. Bencivenni,¹⁹ S. Benson,²⁸ S. Beranek,¹⁰ A. Berezhnoy,³⁵ R. Bernet,⁴⁶ D. Berninghoff,¹³ E. Bertholet,⁹ A. Bertolin,²⁴ C. Betancourt,⁴⁶ F. Betti,^{16,c} M. O. Bettler,⁵¹ M. van Beuzekom,²⁸ I. Bezshyiko,⁴⁶ S. Bhasin,⁵⁰ J. Bhom,³⁰ M. S. Bieker,¹¹ S. Bifani,⁴⁹ P. Billoir,⁹ A. Birnkraut,¹¹ A. Bizzeti,^{18,d} M. Björn,⁵⁹ M. P. Blago,⁴⁴ T. Blake,⁵² F. Blanc,⁴⁵ S. Blusk,⁶³ D. Bobulska,⁵⁵ V. Bocci,²⁷ O. Boente Garcia,⁴³ T. Boettcher,⁶⁰ A. Bondar,^{39,e} N. Bondar,⁴¹ S. Borghi,^{58,44} M. Borisyak,³⁷ M. Borsato,¹³ M. Boubdir,¹⁰ T. J. V. Bowcock,⁵⁶ C. Bozzi,^{17,44} S. Braun,¹³ A. Brea Rodriguez,⁴³ M. Brodski,⁴⁴ J. Brodzicka,³⁰ A. Brossa Gonzalo,⁵² D. Brundu,^{23,44} E. Buchanan,⁵⁰ A. Buonaura,⁴⁶ C. Burr,⁵⁸ A. Bursche,²³ J. S. Butter,²⁸ J. Buytaert,⁴⁴ W. Byczynski,⁴⁴ S. Cadetdu,²³ H. Cai,⁶⁸ R. Calabrese,^{17,f} S. Cali,¹⁹ R. Calladine,⁴⁹ M. Calvi,^{21,b} M. Calvo Gomez,^{42,g} A. Camboni,^{42,g} P. Campana,¹⁹ D. H. Campora Perez,⁴⁴ L. Capriotti,^{16,c} A. Carbone,^{16,c} G. Carboni,²⁶ R. Cardinale,²⁰ A. Cardini,²³ P. Carniti,^{21,b} K. Carvalho Akiba,² A. Casais Vidal,⁴³ G. Casse,⁵⁶ M. Cattaneo,⁴⁴ G. Cavallero,²⁰ R. Cenci,^{25,h} M. G. Chapman,⁵⁰ M. Charles,^{9,44} Ph. Charpentier,⁴⁴ G. Chatzikonstantinidis,⁴⁹ M. Chefdeville,⁵ V. Chekalina,³⁷ C. Chen,³ S. Chen,²³ S.-G. Chitic,⁴⁴ V. Chobanova,⁴³ M. Chruszcz,⁴⁴ A. Chubykin,⁴¹ P. Ciambone,¹⁹ X. Cid Vidal,⁴³ G. Ciezarek,⁴⁴ F. Cindolo,¹⁶ P. E. L. Clarke,⁵⁴ M. Clemencic,⁴⁴ H. V. Cliff,⁵¹ J. Closier,⁴⁴ V. Coco,⁴⁴ J. A. B. Coelho,⁸ J. Cogan,⁷ E. Cogneras,⁶ L. Cojocariu,³³ P. Collins,⁴⁴ T. Colombo,⁴⁴ A. Comerma-Montells,¹³ A. Contu,²³ G. Coombs,⁴⁴ S. Coquereau,⁴² G. Corti,⁴⁴ C. M. Costa Sobral,⁵² B. Couturier,⁴⁴ G. A. Cowan,⁵⁴ D. C. Craik,⁶⁰ A. Crocombe,⁵² M. Cruz Torres,¹ R. Currie,⁵⁴ C. D'Ambrosio,⁴⁴ C. L. Da Silva,⁸¹ E. Dall'Occo,²⁸ J. Dalseno,^{43,dd} A. Danilina,³⁴ A. Davis,⁵⁸ O. De Aguiar Francisco,⁴⁴ K. De Bruyn,⁴⁴ S. De Capua,⁵⁸ M. De Cian,⁴⁵ J. M. De Miranda,¹ L. De Paula,² M. De Serio,^{15,i} P. De Simone,¹⁹ C. T. Dean,⁵⁵ W. Dean,⁷⁹ D. Decamp,⁵ L. Del Buono,⁹ B. Delaney,⁵¹ H.-P. Dembinski,¹² M. Demmer,¹¹ A. Dendek,³¹ D. Derkach,³⁸ O. Deschamps,⁶ F. Desse,⁸ F. Dettori,²³ B. Dey,⁶⁹ A. Di Canto,⁴⁴ P. Di Nezza,¹⁹ S. Didenko,⁷⁶ H. Dijkstra,⁴⁴ F. Dordei,²³ M. Dorigo,^{25,j} A. Dosil Suárez,⁴³ L. Douglas,⁵⁵ A. Dovbnya,⁴⁷ K. Dreimanis,⁵⁶ L. Dufour,⁴⁴ G. Dujany,⁹ P. Durante,⁴⁴ J. M. Durham,⁸¹ D. Dutta,⁵⁸ R. Dzhelyadin,⁴⁰ M. Dziewiecki,¹³ A. Dziurda,³⁰ A. Dzyuba,⁴¹ S. Easo,⁵³ U. Egede,⁵⁷ V. Egorychev,³⁴ S. Eidelman,^{39,e} S. Eisenhardt,⁵⁴ U. Eitschberger,¹¹ S. Ek-In,⁴⁵ R. Ekelhof,¹¹ L. Eklund,⁵⁵ S. Ely,⁶³ A. Ene,³³ S. Escher,¹⁰ S. Esen,²⁸ T. Evans,⁶¹ A. Falabella,¹⁶ N. Farley,⁴⁹ S. Farry,⁵⁶ D. Fazzini,⁸ P. Fernandez Declara,⁴⁴ A. Fernandez Prieto,⁴³ C. Fernández-Ramírez,⁷³ F. Ferrari,^{16,c} L. Ferreira Lopes,⁴⁵ F. Ferreira Rodrigues,² S. Ferreres Sole,²⁸ M. Ferro-Luzzi,⁴⁴ S. Filippov,³⁶ R. A. Fini,¹⁵ M. Fiorini,^{17,f} M. Firlej,³¹ C. Fitzpatrick,⁴⁴ T. Fiutowski,³¹ F. Fleuret,^{8,a} M. Fontana,⁴⁴ F. Fontanelli,^{20,k} R. Forty,⁴⁴ V. Franco Lima,⁵⁶ M. Franco Sevilla,⁶² M. Frank,⁴⁴ C. Frei,⁴⁴ J. Fu,^{22,l} W. Funk,⁴⁴ C. Färber,⁴⁴ M. Féo,⁴⁴ E. Gabriel,⁵⁴ A. Gallas Torreira,⁴³ D. Galli,^{16,c} S. Gallorini,²⁴ S. Gambetta,⁵⁴ Y. Gan,³ M. Gandelman,² P. Gandini,²² Y. Gao,³ L. M. Garcia Martin,⁷⁸ B. Garcia Plana,⁴³ J. García Pardiñas,⁴⁶ J. Garra Tico,⁵¹ L. Garrido,⁴² D. Gascon,⁴² C. Gaspar,⁴⁴ G. Gazzoni,⁶ D. Gerick,¹³ E. Gersabeck,⁵⁸ M. Gersabeck,⁵⁸ T. Gershon,⁵² D. Gerstel,⁷ Ph. Ghez,⁵ V. Gibson,⁵¹ O. G. Girard,⁴⁵ P. Gironella Gironell,⁴² L. Giubega,³³ K. Gizdov,⁵⁴ V. V. Gligorov,⁹ D. Golubkov,³⁴ A. Golutvin,^{57,76} A. Gomes,^{1,m} I. V. Gorelov,³⁵ C. Gotti,^{21,b} E. Govorkova,²⁸ J. P. Grabowski,¹³ R. Graciani Diaz,⁴² L. A. Granado Cardoso,⁴⁴ E. Graugés,⁴² E. Graverini,⁴⁵ G. Graziani,¹⁸ A. Grecu,³³ R. Greim,²⁸ P. Griffith,²³ L. Grillo,⁵⁸ L. Gruber,⁴⁴ B. R. Gruber Cazon,⁵⁹ C. Gu,³ X. Guo,⁶⁷ E. Gushchin,³⁶ A. Guth,¹⁰ Yu. Guz,^{40,44} T. Gys,⁴⁴ C. Göbel,⁶⁵ T. Hadavizadeh,⁵⁹ C. Hadjivasiliou,⁶ G. Haefeli,⁴⁵ C. Haen,⁴⁴ S. C. Haines,⁵¹ B. Hamilton,⁶² Q. Han,⁶⁹ X. Han,¹³ T. H. Hancock,⁵⁹ S. Hansmann-Menzemer,¹³ N. Harnew,⁵⁹ T. Harrison,⁵⁶

C. Hasse,⁴⁴ M. Hatch,⁴⁴ J. He,⁶⁶ M. Hecker,⁵⁷ K. Heinicke,¹¹ A. Heister,¹¹ K. Hennessy,⁵⁶ L. Henry,⁷⁸ E. van Herwijnen,⁴⁴ J. Heuel,¹⁰ M. Heß,⁷¹ A. Hicheur,⁶⁴ R. Hidalgo Charman,⁵⁸ D. Hill,⁵⁹ M. Hilton,⁵⁸ P. H. Hopchev,⁴⁵ J. Hu,¹³ W. Hu,⁶⁹ W. Huang,⁶⁶ Z. C. Huard,⁶¹ W. Hulsbergen,²⁸ T. Humair,⁵⁷ M. Hushchyn,³⁸ D. Hutchcroft,⁵⁶ D. Hynds,²⁸ P. Ibis,¹¹ M. Idzik,³¹ P. Ilten,⁴⁹ A. Inglessi,⁴¹ A. Inyakin,⁴⁰ K. Ivshin,⁴¹ R. Jacobsson,⁴⁴ S. Jakobsen,⁴⁴ J. Jalocha,⁵⁹ E. Jans,²⁸ B. K. Jashal,⁷⁸ A. Jawahery,⁶² F. Jiang,³ M. John,⁵⁹ D. Johnson,⁴⁴ C. R. Jones,⁵¹ C. Joram,⁴⁴ B. Jost,⁴⁴ N. Jurik,⁵⁹ S. Kandybei,⁴⁷ M. Karacson,⁴⁴ J. M. Kariuki,⁵⁰ S. Karodia,⁵⁵ N. Kazeev,³⁸ M. Kecke,¹³ F. Keizer,⁵¹ M. Kelsey,⁶³ M. Kenzie,⁵¹ T. Ketel,²⁹ B. Khanji,⁴⁴ A. Kharisova,⁷⁷ C. Khurewathanakul,⁴⁵ K. E. Kim,⁶³ T. Kim,¹⁰ V. S. Kirsebom,⁴⁵ S. Klaver,¹⁹ K. Klimaszewski,³² S. Koliiev,⁴⁸ M. Kolpin,¹³ A. Kondybayeva,⁷⁶ A. Konoplyannikov,³⁴ R. Kopecna,¹³ P. Koppenburg,²⁸ I. Kostiuik,^{28,48} O. Kot,⁴⁸ S. Kotriakhova,⁴¹ M. Kozeiha,⁶ L. Kravchuk,³⁶ M. Kreps,⁵² F. Kress,⁵⁷ S. Kretzschmar,¹⁰ P. Krokovny,^{39,e} W. Krupa,³¹ W. Krzemien,³² W. Kucewicz,^{30,n} M. Kucharczyk,³⁰ V. Kudryavtsev,^{39,e} G. J. Kunde,⁸¹ A. K. Kuonen,⁴⁵ T. Kvaratskheliya,³⁴ D. Lacarrere,⁴⁴ G. Lafferty,⁵⁸ A. Lai,²³ D. Lancierini,⁴⁶ G. Lanfranchi,¹⁹ C. Langenbruch,¹⁰ T. Latham,⁵² C. Lazzeroni,⁴⁹ R. Le Gac,⁷ A. Leflat,³⁵ R. Lefèvre,⁶ F. Lemaître,⁴⁴ O. Leroy,⁷ T. Lesiak,³⁰ B. Leverington,¹³ H. Li,⁶⁷ P.-R. Li,^{66,o} X. Li,⁸¹ Y. Li,⁴ Z. Li,⁶³ X. Liang,⁶³ T. Likhomanenko,⁷⁵ R. Lindner,⁴⁴ P. Ling,⁶⁷ F. Lionetto,⁴⁶ V. Lisovskyi,⁸ G. Liu,⁶⁷ X. Liu,³ D. Loh,⁵² A. Loi,²³ J. Lomba Castro,⁴³ I. Longstaff,⁵⁵ J. H. Lopes,² G. Loustau,⁴⁶ G. H. Lovell,⁵¹ D. Lucchesi,^{24,p} M. Lucio Martinez,⁴³ Y. Luo,³ A. Lupato,²⁴ E. Luppi,^{17,f} O. Lupton,⁵² A. Lusiani,²⁵ X. Lyu,⁶⁶ R. Ma,⁶⁷ F. Machefert,⁸ F. Maciuc,³³ V. Macko,⁴⁵ P. Mackowiak,¹¹ S. Maddrell-Mander,⁵⁰ O. Maev,^{41,44} K. Maguire,⁵⁸ D. Maisuzenko,⁴¹ M. W. Majewski,³¹ S. Malde,⁵⁹ B. Malecki,⁴⁴ A. Malinin,⁷⁵ T. Maltsev,^{39,e} H. Malygina,¹³ G. Manca,^{23,q} G. Mancinelli,⁷ D. Marangotto,^{22,1} J. Maratas,^{6,r} J. F. Marchand,⁵ U. Marconi,¹⁶ C. Marin Benito,⁸ M. Marinangeli,⁴⁵ P. Marino,⁴⁵ J. Marks,¹³ P. J. Marshall,⁵⁶ G. Martellotti,²⁷ L. Martinazzoli,⁴⁴ M. Martinelli,^{44,21} D. Martinez Santos,⁴³ F. Martinez Vidal,⁷⁸ A. Massafferri,¹ M. Materok,¹⁰ R. Matev,⁴⁴ A. Mathad,⁴⁶ Z. Mathe,⁴⁴ V. Matiunin,³⁴ C. Matteuzzi,²¹ K. R. Mattioli,⁷⁹ A. Mauri,⁴⁶ E. Maurice,^{8,a} B. Maurin,⁴⁵ M. McCann,^{57,44} A. McNab,⁵⁸ R. McNulty,¹⁴ J. V. Mead,⁵⁶ B. Meadows,⁶¹ C. Meaux,⁷ N. Meinert,⁷¹ D. Melnychuk,³² M. Merk,²⁸ A. Merli,^{22,1} E. Michielin,²⁴ M. Mikhasenko,⁴⁴ D. A. Milanese,⁷⁰ E. Millard,⁵² M.-N. Minard,⁵ L. Minzoni,^{17,f} D. S. Mitzel,¹³ A. Mogini,⁹ R. D. Moise,⁵⁷ T. Mombächer,¹¹ I. A. Monroy,⁷⁰ S. Monteil,⁶ M. Morandin,²⁴ G. Morello,¹⁹ M. J. Morello,^{25,s} J. Moron,³¹ A. B. Morris,⁷ R. Mountain,⁶³ H. Mu,³ F. Muheim,⁵⁴ M. Mukherjee,⁶⁹ M. Mulder,²⁸ C. H. Murphy,⁵⁹ D. Murray,⁵⁸ A. Mödden,¹¹ D. Müller,⁴⁴ J. Müller,¹¹ K. Müller,⁴⁶ V. Müller,¹¹ P. Naik,⁵⁰ T. Nakada,⁴⁵ R. Nandakumar,⁵³ A. Nandi,⁵⁹ T. Nanut,⁴⁵ I. Nasteva,² M. Needham,⁵⁴ N. Neri,^{22,1} S. Neubert,¹³ N. Neufeld,⁴⁴ R. Newcombe,⁵⁷ T. D. Nguyen,⁴⁵ C. Nguyen-Mau,^{45,t} S. Nieswand,¹⁰ R. Niet,¹¹ N. Nikitin,³⁵ N. S. Nolte,⁴⁴ D. P. O'Hanlon,¹⁶ A. Oblakowska-Mucha,³¹ V. Obraztsov,⁴⁰ S. Ogilvy,⁵⁵ R. Oldeman,^{23,q} C. J. G. Onderwater,⁷⁴ J. D. Osborn,⁷⁹ A. Ossowska,³⁰ J. M. Otalora Goicochea,² T. Ovsiannikova,³⁴ P. Owen,⁴⁶ A. Oyanguren,⁷⁸ P. R. Pais,⁴⁵ T. Pajero,^{25,s} A. Palano,¹⁵ M. Palutan,¹⁹ G. Panshin,⁷⁷ A. Papanestis,⁵³ M. Pappagallo,⁵⁴ L. L. Pappalardo,^{17,f} W. Parker,⁶² C. Parkes,^{58,44} G. Passaleva,^{18,44} A. Pastore,¹⁵ M. Patel,⁵⁷ C. Patrignani,^{16,c} A. Pearce,⁴⁴ A. Pellegrino,²⁸ G. Penso,²⁷ M. Pepe Altarelli,⁴⁴ S. Perazzini,¹⁶ D. Pereima,³⁴ P. Perret,⁶ L. Pescatore,⁴⁵ K. Petridis,⁵⁰ A. Petrolini,^{20,k} A. Petrov,⁷⁵ S. Petrucci,⁵⁴ M. Petruzzo,^{22,1} B. Pietrzyk,⁵ G. Pietrzyk,⁴⁵ M. Piques,³⁰ M. Pili,⁵⁹ A. Pilloni,^{72,u} D. Pinci,²⁷ J. Pinzino,⁴⁴ F. Pisani,⁴⁴ A. Piucci,¹³ V. Placinta,³³ S. Playfer,⁵⁴ J. Plews,⁴⁹ M. Plo Casasus,⁴³ F. Polci,⁹ M. Poli Lener,¹⁹ M. Poliakov,⁶³ A. Poluektov,⁷ N. Polukhina,^{76,v} I. Polyakov,⁶³ E. Polcarpo,² G. J. Pomery,⁵⁰ S. Ponce,⁴⁴ A. Popov,⁴⁰ D. Popov,⁴⁹ S. Poslavskii,⁴⁰ E. Price,⁵⁰ C. Prouve,⁴³ V. Pugatch,⁴⁸ A. Puig Navarro,⁴⁶ H. Pullen,⁵⁹ G. Punzi,^{25,h} W. Qian,⁶⁶ J. Qin,⁶⁶ R. Quagliani,⁹ B. Quintana,⁶ N. V. Raab,¹⁴ B. Rachwal,³¹ J. H. Rademacker,⁵⁰ M. Rama,²⁵ M. Ramos Pernas,⁴³ M. S. Rangel,² F. Ratnikov,^{37,38} G. Raven,²⁹ M. Ravonel Salzgeber,⁴⁴ M. Reboud,⁵ F. Redi,⁴⁵ S. Reichert,¹¹ A. C. dos Reis,¹ F. Reiss,⁹ C. Remon Alepuz,⁷⁸ Z. Ren,³ V. Renaudin,⁵⁹ S. Ricciardi,⁵³ S. Richards,⁵⁰ K. Rinnert,⁵⁶ P. Robbe,⁸ A. Robert,⁹ A. B. Rodrigues,⁴⁵ E. Rodrigues,⁶¹ J. A. Rodriguez Lopez,⁷⁰ M. Roehrken,⁴⁴ S. Roiser,⁴⁴ A. Rollings,⁵⁹ V. Romanovskiy,⁴⁰ A. Romero Vidal,⁴³ J. D. Roth,⁷⁹ M. Rotondo,¹⁹ M. S. Rudolph,⁶³ T. Ruf,⁴⁴ J. Ruiz Vidal,⁷⁸ J. J. Saborido Silva,⁴³ N. Sagidova,⁴¹ B. Saitta,^{23,q} V. Salustino Guimaraes,⁶⁵ C. Sanchez Gras,²⁸ C. Sanchez Mayordomo,⁷⁸ B. Sanmartin Sedes,⁴³ R. Santacesaria,²⁷ C. Santamarina Rios,⁴³ M. Santimaria,^{19,44} E. Santovetti,^{26,w} G. Sarpis,⁵⁸ A. Sarti,^{19,x} C. Satriano,^{27,y} A. Satta,²⁶ M. Saur,⁶⁶ D. Savrina,^{34,35} S. Schael,¹⁰ M. Schellenberg,¹¹ M. Schiller,⁵⁵ H. Schindler,⁴⁴ M. Schmelling,¹² T. Schmelzer,¹¹ B. Schmidt,⁴⁴ O. Schneider,⁴⁵ A. Schopper,⁴⁴ H. F. Schreiner,⁶¹ M. Schubiger,²⁸ S. Schulte,⁴⁵ M. H. Schune,⁸ R. Schwemmer,⁴⁴ B. Sciascia,¹⁹ A. Sciubba,^{27,x} A. Semennikov,³⁴ E. S. Sepulveda,⁹ A. Sergi,^{49,44} N. Serra,⁴⁶ J. Serrano,⁷ L. Sestini,²⁴ A. Seuthe,¹¹ P. Seyfert,⁴⁴ M. Shapkin,⁴⁰ T. Shears,⁵⁶ L. Shekhtman,^{39,e} V. Shevchenko,⁷⁵ E. Shmanin,⁷⁶ B. G. Siddi,¹⁷ R. Silva Coutinho,⁴⁶ L. Silva de Oliveira,² G. Simi,^{24,p} S. Simone,^{15,i} I. Skiba,¹⁷ N. Skidmore,¹³

T. Skwarnicki,⁶³ M. W. Slater,⁴⁹ J. G. Smeaton,⁵¹ E. Smith,¹⁰ I. T. Smith,⁵⁴ M. Smith,⁵⁷ M. Soares,¹⁶ I. Soares Lavra,¹ M. D. Sokoloff,⁶¹ F. J. P. Soler,⁵⁵ B. Souza De Paula,² B. Spaan,¹¹ E. Spadaro Norella,^{22,1} P. Spradlin,⁵⁵ F. Stagni,⁴⁴ M. Stahl,¹³ S. Stahl,⁴⁴ P. Stefko,⁴⁵ S. Stefkova,⁵⁷ O. Steinkamp,⁴⁶ S. Stemmler,¹³ O. Stenyakin,⁴⁰ M. Stepanova,⁴¹ H. Stevens,¹¹ A. Stocchi,⁸ S. Stone,⁶³ S. Stracka,²⁵ M. E. Stramaglia,⁴⁵ M. Straticiu,³³ U. Straumann,⁴⁶ S. Strovov,⁷⁷ J. Sun,³ L. Sun,⁶⁸ Y. Sun,⁶² K. Swientek,³¹ A. Szabelski,³² A. Szczepaniak,^{80,z} T. Szumlak,³¹ M. Szymanski,⁶⁶ S. T'Jampens,⁵ Z. Tang,³ T. Tekampe,¹¹ G. Tellarini,¹⁷ F. Teubert,⁴⁴ E. Thomas,⁴⁴ J. van Tilburg,²⁸ M. J. Tilley,⁵⁷ V. Tisserand,⁶ M. Tobin,⁴ S. Tolch,⁴⁴ L. Tomassetti,^{17,f} D. Tonelli,²⁵ D. Y. Tou,⁹ E. Tournefier,⁵ M. Traill,⁵⁵ M. T. Tran,⁴⁵ A. Trisovic,⁵¹ A. Tsaregorodtsev,⁷ G. Tuci,^{25,44,h} A. Tully,⁵¹ N. Tuning,²⁸ A. Ukleja,³² A. Usachov,⁸ A. Ustyuzhanin,^{37,38} U. Uwer,¹³ A. Vagner,⁷⁷ V. Vagnoni,¹⁶ A. Valassi,⁴⁴ S. Valat,⁴⁴ G. Valenti,¹⁶ H. Van Hecke,⁸¹ C. B. Van Hulse,¹⁴ A. Vasiliev,⁴⁰ R. Vazquez Gomez,⁴⁴ P. Vazquez Regueiro,⁴³ S. Vecchi,¹⁷ M. van Veghel,²⁸ J. J. Velthuis,⁵⁰ M. Veltri,^{18,aa} A. Venkateswaran,⁶³ M. Vernet,⁶ M. Veronesi,²⁸ M. Vesterinen,⁵² J. V. Viana Barbosa,⁴⁴ D. Vieira,⁶⁶ M. Vieites Diaz,⁴³ H. Viemann,⁷¹ X. Vilasis-Cardona,^{42,g} A. Vitkovskiy,²⁸ M. Vitti,⁵¹ V. Volkov,³⁵ A. Vollhardt,⁴⁶ D. Vom Bruch,⁹ B. Voneki,⁴⁴ A. Vorobyev,⁴¹ V. Vorobyev,^{39,e} N. Voropaev,⁴¹ J. A. de Vries,²⁸ C. Vázquez Sierra,²⁸ R. Waldi,⁷¹ J. Walsh,²⁵ J. Wang,⁴ J. Wang,³ M. Wang,³ Y. Wang,⁶⁹ Z. Wang,⁴⁶ D. R. Ward,⁵¹ H. M. Wark,⁵⁶ N. K. Watson,⁴⁹ D. Websdale,⁵⁷ A. Weiden,⁴⁶ C. Weisser,⁶⁰ M. Whitehead,¹⁰ G. Wilkinson,⁵⁹ M. Wilkinson,⁶³ I. Williams,⁵¹ M. R. J. Williams,⁵⁸ M. Williams,⁶⁰ T. Williams,⁴⁹ F. F. Wilson,⁵³ M. Winn,⁸ W. Wislicki,³² M. Witek,³⁰ G. Wormser,⁸ S. A. Wotton,⁵¹ K. Wyllie,⁴⁴ D. Xiao,⁶⁹ Y. Xie,⁶⁹ H. Xing,⁶⁷ A. Xu,³ L. Xu,³ M. Xu,⁶⁹ Q. Xu,⁶⁶ Z. Xu,³ Z. Xu,⁵ Z. Yang,³ Z. Yang,⁶² Y. Yao,⁶³ L. E. Yeomans,⁵⁶ H. Yin,⁶⁹ J. Yu,^{69,bb} X. Yuan,⁶³ O. Yushchenko,⁴⁰ K. A. Zarebski,⁴⁹ M. Zavertyaev,^{12,v} M. Zeng,³ D. Zhang,⁶⁹ L. Zhang,³ S. Zhang,³ W. C. Zhang,^{3,cc} Y. Zhang,⁴⁴ A. Zhelezov,¹³ Y. Zheng,⁶⁶ X. Zhu,³ V. Zhukov,^{10,35} J. B. Zonneveld,⁵⁴ and S. Zucchelli^{16,c}

(LHCb Collaboration)

¹Centro Brasileiro de Pesquisas Físicas (CBPF), Rio de Janeiro, Brazil

²Universidade Federal do Rio de Janeiro (UFRJ), Rio de Janeiro, Brazil

³Center for High Energy Physics, Tsinghua University, Beijing, China

⁴Institute Of High Energy Physics (ihep), Beijing, China

⁵Univ. Grenoble Alpes, Univ. Savoie Mont Blanc, CNRS, IN2P3-LAPP, Annecy, France

⁶Université Clermont Auvergne, CNRS/IN2P3, LPC, Clermont-Ferrand, France

⁷Aix Marseille Univ, CNRS/IN2P3, CPPM, Marseille, France

⁸LAL, Univ. Paris-Sud, CNRS/IN2P3, Université Paris-Saclay, Orsay, France

⁹LPNHE, Sorbonne Université, Paris Diderot Sorbonne Paris Cité, CNRS/IN2P3, Paris, France

¹⁰I. Physikalisches Institut, RWTH Aachen University, Aachen, Germany

¹¹Fakultät Physik, Technische Universität Dortmund, Dortmund, Germany

¹²Max-Planck-Institut für Kernphysik (MPIK), Heidelberg, Germany

¹³Physikalisches Institut, Ruprecht-Karls-Universität Heidelberg, Heidelberg, Germany

¹⁴School of Physics, University College Dublin, Dublin, Ireland

¹⁵INFN Sezione di Bari, Bari, Italy

¹⁶INFN Sezione di Bologna, Bologna, Italy

¹⁷INFN Sezione di Ferrara, Ferrara, Italy

¹⁸INFN Sezione di Firenze, Firenze, Italy

¹⁹INFN Laboratori Nazionali di Frascati, Frascati, Italy

²⁰INFN Sezione di Genova, Genova, Italy

²¹INFN Sezione di Milano-Bicocca, Milano, Italy

²²INFN Sezione di Milano, Milano, Italy

²³INFN Sezione di Cagliari, Monserrato, Italy

²⁴INFN Sezione di Padova, Padova, Italy

²⁵INFN Sezione di Pisa, Pisa, Italy

²⁶INFN Sezione di Roma Tor Vergata, Roma, Italy

²⁷INFN Sezione di Roma La Sapienza, Roma, Italy

²⁸Nikhef National Institute for Subatomic Physics, Amsterdam, Netherlands

²⁹Nikhef National Institute for Subatomic Physics and VU University Amsterdam, Amsterdam, Netherlands

³⁰Henryk Niewodniczanski Institute of Nuclear Physics Polish Academy of Sciences, Kraków, Poland

³¹AGH—University of Science and Technology, Faculty of Physics and Applied Computer Science, Kraków, Poland

- ³²National Center for Nuclear Research (NCBJ), Warsaw, Poland
- ³³Horia Hulubei National Institute of Physics and Nuclear Engineering, Bucharest-Magurele, Romania
- ³⁴Institute of Theoretical and Experimental Physics NRC Kurchatov Institute (ITEP NRC KI), Moscow, Russia, Moscow, Russia
- ³⁵Institute of Nuclear Physics, Moscow State University (SINP MSU), Moscow, Russia
- ³⁶Institute for Nuclear Research of the Russian Academy of Sciences (INR RAS), Moscow, Russia
- ³⁷Yandex School of Data Analysis, Moscow, Russia
- ³⁸National Research University Higher School of Economics, Moscow, Russia
- ³⁹Budker Institute of Nuclear Physics (SB RAS), Novosibirsk, Russia
- ⁴⁰Institute for High Energy Physics NRC Kurchatov Institute (IHEP NRC KI), Protvino, Russia, Protvino, Russia
- ⁴¹Petersburg Nuclear Physics Institute NRC Kurchatov Institute (PNPI NRC KI), Gatchina, Russia, St.Petersburg, Russia
- ⁴²ICCUB, Universitat de Barcelona, Barcelona, Spain
- ⁴³Instituto Galego de Física de Altas Enerxías (IGFAE), Universidade de Santiago de Compostela, Santiago de Compostela, Spain
- ⁴⁴European Organization for Nuclear Research (CERN), Geneva, Switzerland
- ⁴⁵Institute of Physics, Ecole Polytechnique Fédérale de Lausanne (EPFL), Lausanne, Switzerland
- ⁴⁶Physik-Institut, Universität Zürich, Zürich, Switzerland
- ⁴⁷NSC Kharkiv Institute of Physics and Technology (NSC KIPT), Kharkiv, Ukraine
- ⁴⁸Institute for Nuclear Research of the National Academy of Sciences (KINR), Kyiv, Ukraine
- ⁴⁹University of Birmingham, Birmingham, United Kingdom
- ⁵⁰H.H. Wills Physics Laboratory, University of Bristol, Bristol, United Kingdom
- ⁵¹Cavendish Laboratory, University of Cambridge, Cambridge, United Kingdom
- ⁵²Department of Physics, University of Warwick, Coventry, United Kingdom
- ⁵³STFC Rutherford Appleton Laboratory, Didcot, United Kingdom
- ⁵⁴School of Physics and Astronomy, University of Edinburgh, Edinburgh, United Kingdom
- ⁵⁵School of Physics and Astronomy, University of Glasgow, Glasgow, United Kingdom
- ⁵⁶Oliver Lodge Laboratory, University of Liverpool, Liverpool, United Kingdom
- ⁵⁷Imperial College London, London, United Kingdom
- ⁵⁸School of Physics and Astronomy, University of Manchester, Manchester, United Kingdom
- ⁵⁹Department of Physics, University of Oxford, Oxford, United Kingdom
- ⁶⁰Massachusetts Institute of Technology, Cambridge, Massachusetts, USA
- ⁶¹University of Cincinnati, Cincinnati, Ohio, USA
- ⁶²University of Maryland, College Park, Maryland, USA
- ⁶³Syracuse University, Syracuse, New York, USA
- ⁶⁴Laboratory of Mathematical and Subatomic Physics, Constantine, Algeria
[associated with Universidade Federal do Rio de Janeiro (UFRJ), Rio de Janeiro, Brazil]
- ⁶⁵Pontifícia Universidade Católica do Rio de Janeiro (PUC-Rio), Rio de Janeiro, Brazil
[associated with Universidade Federal do Rio de Janeiro (UFRJ), Rio de Janeiro, Brazil]
- ⁶⁶University of Chinese Academy of Sciences, Beijing, China (associated with Center for High Energy Physics, Tsinghua University, Beijing, China)
- ⁶⁷South China Normal University, Guangzhou, China (associated with Center for High Energy Physics, Tsinghua University, Beijing, China)
- ⁶⁸School of Physics and Technology, Wuhan University, Wuhan, China (associated with Center for High Energy Physics, Tsinghua University, Beijing, China)
- ⁶⁹Institute of Particle Physics, Central China Normal University, Wuhan, Hubei, China
(associated with Center for High Energy Physics, Tsinghua University, Beijing, China)
- ⁷⁰Departamento de Física, Universidad Nacional de Colombia, Bogota, Colombia (associated with LPNHE, Sorbonne Université, Paris Diderot Sorbonne Paris Cité, CNRS/IN2P3, Paris, France)
- ⁷¹Institut für Physik, Universität Rostock, Rostock, Germany (associated with Physikalisches Institut, Ruprecht-Karls-Universität Heidelberg, Heidelberg, Germany)
- ⁷²European Centre for Theoretical Studies in Nuclear Physics and Related Areas and Fondazione Bruno Kessler, Villazzano, Italy
- ⁷³Universidad Nacional Autónoma de México, Ciudad de México, Mexico
- ⁷⁴Van Swinderen Institute, University of Groningen, Groningen, Netherlands
(associated with Nikhef National Institute for Subatomic Physics, Amsterdam, Netherlands)
- ⁷⁵National Research Centre Kurchatov Institute, Moscow, Russia [associated with Institute of Theoretical and Experimental Physics NRC Kurchatov Institute (ITEP NRC KI), Moscow, Russia, Moscow, Russia]
- ⁷⁶National University of Science and Technology “MISIS”, Moscow, Russia [associated with Institute of Theoretical and Experimental Physics NRC Kurchatov Institute (ITEP NRC KI), Moscow, Russia, Moscow, Russia]
- ⁷⁷National Research Tomsk Polytechnic University, Tomsk, Russia [associated with Institute of Theoretical and Experimental Physics NRC Kurchatov Institute (ITEP NRC KI), Moscow, Russia, Moscow, Russia]
- ⁷⁸Instituto de Física Corpuscular, Centro Mixto Universidad de Valencia—CSIC, Valencia, Spain
(associated with ICCUB, Universitat de Barcelona, Barcelona, Spain)

⁷⁹*University of Michigan, Ann Arbor, USA (associated with Syracuse University, Syracuse, New York, USA)*

⁸⁰*Indiana University, Bloomington, USA*

⁸¹*Los Alamos National Laboratory (LANL), Los Alamos, USA (associated with Syracuse University, Syracuse, New York, USA)*

^aAlso at Laboratoire Leprince-Ringuet, Palaiseau, France.

^bAlso at Università di Milano Bicocca, Milano, Italy.

^cAlso at Università di Bologna, Bologna, Italy.

^dAlso at Università di Modena e Reggio Emilia, Modena, Italy.

^eAlso at Novosibirsk State University, Novosibirsk, Russia.

^fAlso at Università di Ferrara, Ferrara, Italy.

^gAlso at LIFAELS, La Salle, Universitat Ramon Llull, Barcelona, Spain.

^hAlso at Università di Pisa, Pisa, Italy.

ⁱAlso at Università di Bari, Bari, Italy.

^jAlso at Sezione INFN di Trieste, Trieste, Italy.

^kAlso at Università di Genova, Genova, Italy.

^lAlso at Università degli Studi di Milano, Milano, Italy.

^mAlso at Universidade Federal do Triângulo Mineiro (UFMT), Uberaba-MG, Brazil.

ⁿAlso at AGH—University of Science and Technology, Faculty of Computer Science, Electronics and Telecommunications, Kraków, Poland.

^oAlso at Lanzhou University, Lanzhou, China.

^pAlso at Università di Padova, Padova, Italy.

^qAlso at Università di Cagliari, Cagliari, Italy.

^rAlso at MSU—Iligan Institute of Technology (MSU-IIT), Iligan, Philippines.

^sAlso at Scuola Normale Superiore, Pisa, Italy.

^tAlso at Hanoi University of Science, Hanoi, Vietnam.

^uAlso at INFN Sezione di Genova, Genova, Italy.

^vAlso at P.N. Lebedev Physical Institute, Russian Academy of Science (LPI RAS), Moscow, Russia.

^wAlso at Università di Roma Tor Vergata, Roma, Italy.

^xAlso at Università di Roma La Sapienza, Roma, Italy.

^yAlso at Università della Basilicata, Potenza, Italy.

^zAlso at Thomas Jefferson National Accelerator Facility, Newport News, USA.

^{aa}Also at Università di Urbino, Urbino, Italy.

^{bb}Also at Physics and Micro Electronic College, Hunan University, Changsha City, China.

^{cc}Also at School of Physics and Information Technology, Shaanxi Normal University (SNNU), Xi'an, China.

^{dd}Also at H.H. Wills Physics Laboratory, University of Bristol, Bristol, United Kingdom.